# Optimization of the Czerny–Turner Spectrometer*

ARTHUR B. SHAFER, LAWRENCE R. MEGILL, AND LEANN DROPPLEMAN
*Central Radio Propagation Laboratories, National Bureau of Standards, Boulder, Colorado*
(Received 12 August 1963)

Geometrical optic techniques are used to analyze and compare the symmetrical spherical mirror to the unsymmetrical spherical-mirror Czerny–Turner spectrometer. The aberration problems due to diffraction from the grating are analyzed and methods of partial correction of the aberrations are derived. The flux and resolution advantage of gratings with high blaze angles used in the unsymmetrical spherical-mirror Czerny–Turner is shown. A design and ray tracing routine employing a digital computer is utilized to illustrate the geometric effects of the diffraction grating and the partial corrective measures. Slit curvature is analyzed numerically and some general results are abstracted from the numerical data. It may be inferred from the results of theory and numerical calculations that the unsymmetrical Czerny–Turner spectrometer using two spherical mirrors can be made superior to a similar symmetrical Czerny–Turner spectrometer. A comparison of luminosity is made between the Czerny–Turner spectrometer, utilizing a high blaze grating, and various interferometric and modulating spectrometers and it is shown that the luminosity of the Czerny–Turner spectrometer is comparable or superior.

## I. INTRODUCTION

IT was first recognized by Czerny and Turner,[1] that the aberrations introduced by a spherical collimating mirror $M_1$ can be partially corrected by a symmetrical, but oppositely oriented, spherical condensing mirror $M_2$ (Fig. 1). More recently, Fastie[2] independently designed a spectrometer that was first designed and built by Ebert.[3] Kudo[4] has expanded the Hamilton point-characteristic function for the symmetrical Czerny–Turner, Ebert, and Pfund spectrometers and has given data about slit curvature. Leo[5,6] has shown that because of the change in beam width after diffraction, the original symmetrical arrangement of Czerny and Turner is not satisfactory (see Sec. IV) and has analyzed the problem for the grating[5] and the prism.[6] In all of the work referred to above, except Leo's, it is assumed that the grating has little or no effect upon the quality of the image.

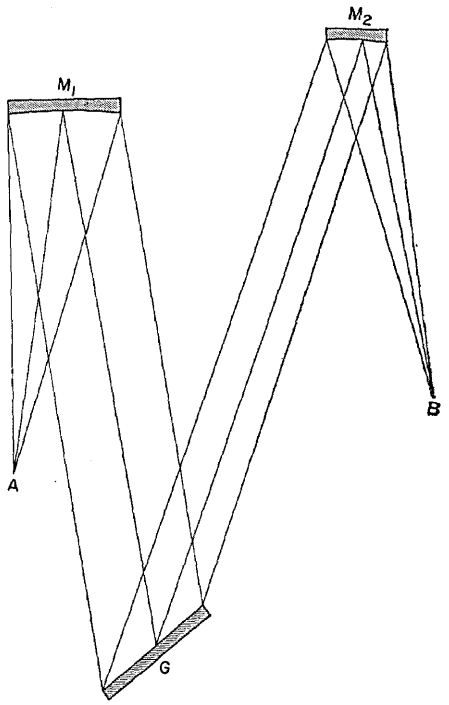


FIG. 1. A two-dimensional schematic of a generalized spherical mirror Czerny–Turner arrangement. A is the entrance slit, B the exit slit. $M_1$ and $M_2$ are the collimating mirror and condensing mirror, respectively. G is the grating. This is not the type of instrument analyzed by M. Czerny and A. F. Turner, since it is asymmetric.

This work, essentially, is an extension and generalization of the work of Leo[5]; we shall take into account (1) the aberration introduced by the collimating mirror, (2) the change in beam width due to the tilt of the grating, (3) the grating or diffraction induced change in the shape of the surface of constant phase, and (4) the amount of, or lack of, correction to the wavefront provided by the second (condensing) mirror.

To obtain analytically the approximate focusing condition and the relative orientation of the slits, mirrors, and grating, use has been made of Hamilton's characteristic $V$ function in two dimensions and Fermat's principle.[7] To obtain a more exact relationship between slits, mirrors and grating, a three-dimensional design and ray trace routine is used, employing a digital computer.

---

* Sections 1, 4, and portions of 5 were presented at the meeting of the Optical Society of America at Los Angeles, California, October 1961; J. Opt. Soc. Am. **51**, 1464 (1961).

[1] M. Czerny and A. F. Turner, Z. Physik. **61**, 792 (1930).

[2] W. G. Fastie, J. Opt. Soc. Am. **42**, 641, 647 (1952).

[3] H. Ebert, Wiedemann Ann. **38**, 489 (1889).

[4] K. Kudo, Sci. Light (Tokyo) **9**, 1 (1960).

[5] W. Leo, Z. Angew. Phys. **8**, 196 (1956).

[6] W. Leo, Z. Instrumentenk. **66**, 240 (1958); **70**, 9 (1962).

[7] W. R. Hamilton, *Mathematical Papers, Geometrical Optics* (Cambridge University Press, London, 1931); Vol. I, Chap. 17, p. 168; J. L. Synge, *Geometrical Optics*, Cambridge University Press (1937); J. L. Synge, *Hamilton's Method in Geometrical Optics* (The Institute for Fluid Dynamics and Applied Mathematics, University of Maryland, College Park, Maryland, 1951); J. L. Synge, J. Opt. Soc. Am. **27**, 75 (1937); M. Herzberger, *ibid.*, p. 133.

## II. FLUX AND RESOLUTION

Several authors[8–13] have written about the flux and/or resolution advantages of the grating with a high-blaze angle (echelle) over a grating with a low-blaze angle (echellette). Some have shown that this advantage is proportional to the sine of the incident or diffraction angle (the angular dispersion) or accrues to the instrument owing to a possible reduction in focal length (possible only if aberrations are ignored). We shall show, on the basis of the excellent work of Jacquinot and Dufour[8] and Jacquinot,[9] that it is larger than shown by previous authors.

The equations for the flux due to a spectral line or a continuum may be written as

$$\Phi = k\tau B_\lambda \delta\lambda (l/F)(2WH \sin\varphi \cos\chi/\lambda), \quad (1)$$

and

$$\Phi = k\tau B_\lambda (\delta\lambda)^2 (l/F)(2WH \sin\varphi \cos\chi/\lambda) \quad (2)$$

where $k$ is a factor related to diffraction by the exit pupil (grating) and the width of the entrance and exit slits,[8,9] $\tau$ is the transmittance of the optical assembly; $B_\lambda$ is the source radiance; $\delta\lambda$, the resolution; $l$, the length of the entrance slit; $F$, the focal length of the collimating mirror; $W$ and $H$ are the width and height of the grating; $\lambda$ is the wavelength; $\varphi$ is the blaze angle; and $\chi$ is the angle between the incoming central ray and the blaze normal or between the central diffracted ray and blaze normal at the blaze wavelengths.

If we wish to maintain the same focal length, aperture, and resolution, but change from a low-blaze to a high-blaze grating, the variables which need to be considered are $W$, $\varphi$, and $k$.

The approximate relation between the width of a high-blaze grating and low-blaze grating is $W_h = W_l(\cos\varphi_l/\cos\varphi_h)$ where the subscript $h$ refers to high blaze and $l$ to low blaze. If $\varphi_l \approx 20°$ and $\varphi_h \approx 76°$ then $\cos\varphi_l/\cos\varphi_h \approx 3.9$, also $\sin\varphi_h/\sin\varphi_l \approx 2.9$. The Rayleigh resolving power of the high-blaze grating is greater by a factor of $\approx 12$ over that of the low-blaze grating; hence, the factor $k$ may increase from $\approx 1.2$ to $\approx 4$. The maximum increase under the above conditions may then be obtained from Eq. (1) or Eq. (2); this is $\Phi_h/\Phi_l \approx 44$; the minimum increase is $\Phi_h/\Phi_l \approx 11$.

It is not possible in all cases to obtain a high-blaze grating wide enough to maintain the aperture. If the low-blaze grating is replaced by a high-blaze grating of the same width, the variables are then $\varphi$ and $k$. Under these conditions the increase in $\varphi$ will give a flux increase of 2.9 (see above) and $k$ will be increased from $\approx 1.2$ to $\approx 3$. The total increase in flux may then be $\approx 3$ to 9.

By considering the possible increase in resolution when using a high-blaze grating, from Eqs. (1) and (2) by keeping the flux constant, $\Phi_l = \Phi_h$, we may write for the line spectra

$$\delta\lambda_h/\delta\lambda_l \approx \sin\varphi_l \cos\varphi_h/\sin\varphi_h \cos\varphi_l, \quad (3)$$

and for the continuum

$$\delta\lambda_h/\delta\lambda_l \approx (\sin\varphi_l \cos\varphi_h/\sin\varphi_h \cos\varphi_l)^{\frac{1}{2}}. \quad (4)$$

Hence the spectral slitwidth, for the same amount of flux, can be reduced.[10]

## III. EFFECT OF THE GRATING UPON WAVEFRONT ABERRATION

Before going into the effect of the grating upon the incident wavefront, it may be well to define three commonly used terms. The image of the entrance slit, formed off-axis by the Czerny–Turner spectrometer, is a structure formed from many types of image aberrations. The common terms such as coma, spherical aberration, or astigmatism usually refer to the third-order Seidel aberrations; but for the case of a spectrometer where a diffraction grating intervenes between the object and image, the usual meaning of these terms is lost. To circumvent the above, the following terms shall be used: (1) *Coma* is an asymmetry of the image of the entrance slit and is orthogonal to the curved exit slit. This will produce an asymmetry of the spread function of the spectrometer and hence an asymmetry in the contour of the observed line. (2) *Astigmatism* is an extension of the image of a point of the entrance slit. The extended point image, if properly curved slits are used, is tangential to the curve of the exit slit. Astigmatism, according to geometrical optics, will have no effect upon the spread function [see Sec. V (b) for probable effects of diffraction]. (3) *Spherical aberration* is a symmetrical spreading of the image of a point of the entrance slit. Spherical aberration will produce a symmetrical broadening of the spread function and hence a widening of the line contour with a possible reduction in resolution or contrast. These terms have the defined meaning throughout this work unless otherwise specified. The effect of the diffraction grating upon the incident wavefront is twofold; it changes the beamwidth and transforms the shape of the incident wavefront. The collimated beamwidth is changed from $W$, before diffraction, to approximately $W\cos\beta_{g0}/\cos\alpha_{g0}$ after diffraction where $\alpha_{g0}$ and $\beta_{g0}$ refer to the incidence and diffraction angles of the central ray. This forces the rays to depart from the conjugate relationship between mirror surfaces of the standard Czerny–Turner condition.[5]

Any aberration in the wavefront produced by the collimating mirror will be transformed by diffraction.

[8] P. Jacquinot and C. Dufour, J. Rech. Centre, Natl. Rech. Sci. Lab, Bellevue (Paris) No. 6, 91 (1948).
[9] P. Jacquinot, J. Opt. Soc. Am. 44, 761 (1954).
[10] G. W. Stroke, J. Opt. Soc. Am. 51, 1321 (1961). Stroke has stressed with the help of numerical values, the advantages in using high-blazed gratings in spectrometers and spectrographs. See also, G. W. Stroke, Progr. Opt. 2, 3 (1963).
[11] V. I. Malyshev and S. G. Rautian, Opt. i Spectroskopiya 6, 550 (1959) [English transl.: Opt. Spectry 6, 351 (1959)].
[12] R. Chabbal, Rev. Opt. 37, 49, 336, 501 (1958).
[13] P. Jacquinot, Rept. Progr. Phys. 23, 267 (1960).

By taking the differential of the diffraction equation

$$n\lambda/d=\cos\psi(\sin\alpha_g+\sin\beta_g),$$

we may obtain, by assuming a small angle variation,

$$\Delta\beta_g=2(\sin\alpha_{g0}/\cos\beta_{g0})\tan\psi\Delta\psi - (\cos\alpha_{g0}/\cos\beta_{g0})\Delta\alpha_g, \quad (5)$$

where $\psi$ is the angle between a plane orthogonal to the face of the grating, the grating rulings and any ray; the angular increments $\Delta\beta_g$, $\Delta\alpha_g$, and $\Delta\psi$ are the derivations of any ray from the central ray angles. An examination of Eq. (5) shows that a symmetrically curved incident wavefront will be diffracted asymmetrically and that an asymmetric wavefront is made more asymmetric.

## IV. APPROXIMATE IMAGING CONDITIONS

The approximate imaging conditions for the Czerny–Turner arrangement will be derived in two dimensions by using Hamilton's characteristic $V$ function and applying Fermat's condition for imaging.

The expansion of the light path function is taken directly from Beutler[14] and reduced to two dimensions giving

$$F=r+r'-w(\sin\alpha+\sin\beta)+\frac{w^2}{2}\left[\left(\frac{\cos^2\alpha}{r}-\frac{\cos\alpha}{R}\right)+\left(\frac{\cos^2\beta}{r'}-\frac{\cos\beta}{R}\right)\right]+\tfrac{1}{2}w^3\left[\frac{\sin\alpha}{r}\left(\frac{\cos^2\alpha}{r}-\frac{\cos\alpha}{R}\right)+\frac{\sin\beta}{r'}\left(\frac{\cos^2\beta}{r'}-\frac{\cos\beta}{R}\right)\right]$$
$$+\tfrac{1}{2}w^4\left[\frac{\sin^2\alpha}{r^2}\left(\frac{\cos^2\alpha}{r}-\frac{\cos\alpha}{R}\right)+\frac{\sin^2\beta}{r'^2}\left(\frac{\cos^2\beta}{r'}-\frac{\cos\beta}{R}\right)\right]+\frac{w^4}{8R^2}\left[\left(\frac{1}{r}-\frac{\cos\alpha}{R}\right)+\left(\frac{1}{r'}-\frac{\cos\beta}{R}\right)\right]+\cdots. \quad (6)$$

In Eq. (6), $R$ is the radius of the mirror, $r$ is the object distance, $r'$ is the image distance, and $\alpha$ and $\beta$ are the angles of incidence and reflection, respectively.

Applying Fermat's principle to Eq. (6) and assuming the central ray approximation where $\beta=-\alpha$, and a collimating condition, $r'=\infty$ we obtain

$$\frac{\partial F}{\partial w}=w\left(\frac{\cos^2\alpha}{r}-\frac{2\cos\alpha}{R}\right)+\tfrac{3}{2}w^2\left(\frac{\sin\alpha\cos^2\alpha}{r^2}-\frac{\sin\alpha\cos\alpha}{rR}\right)$$
$$+2w^3\left(\frac{\sin^2\alpha\cos^2\alpha}{r^3}-\frac{\sin^2\alpha\cos\alpha}{r^2R}\right)+\frac{w^3}{2R^2}\left(\frac{1}{r}-\frac{2\cos\alpha}{R}\right)+\cdots=0. \quad (7)$$

If the first bracket in Eq. (7) is set equal to zero we obtain a central ray solution given by

$$r=r_0=(R/2)\cos\alpha. \quad (8)$$

The path variation for a single surface may be computed from

$$\Delta F_i=\int_0^{w_i}\frac{\partial F}{\partial w}dw, \quad (9)$$

where $w_i$ is a width coordinate of the projection of the grating upon the collimating mirror. If we assume that the aberration is asymmetrical relative to the central ray, i.e.,

$$\int_0^{w_i}\frac{\partial F}{\partial w}dw=-\int_{-w_i}^{0}\frac{\partial F}{\partial w}dw,$$

by using (8), (9), and the second term in (7) we obtain

$$\Delta F_i=\pm(w_i^3/R^2)\sin\alpha. \quad (10)$$

Hence, for the collimating mirror

$$\Delta F_m=\pm(w_m^3/R_1^2)\sin\alpha_m) \quad (11)$$

and for the condensing mirror

$$\Delta F_m'=\mp\frac{w_m'^3}{R_2^2}\sin\alpha_m'. \quad (12)$$

On the assumption that the aberration of the extreme rays is greater than that of the interior rays, correction shall be applied to the extreme rays that strike the grating. The half-width of the second mirror may be expressed as

$$w_m'^3\approx\frac{W_m^3}{8}\frac{\cos^3\beta_g}{\cos^3\alpha_g}\frac{\cos^3\alpha_m}{\cos^3\alpha_m'}. \quad (13)$$

$W_m$ is the projected width of the grating upon the collimating mirror, $\alpha_g$ and $\beta_g$ are angles of incidence and diffraction, $\alpha_m$ and $\alpha_m'$ are the off-axis angles of incidence and reflection of the central ray upon the collimating and condensing mirror. Finally, the desired condition is

$$\Delta F_m+\Delta F_m'=0. \quad (14)$$

[14] H. G. Beutler, J. Opt. Soc. Am. **35**, 311 (1945).

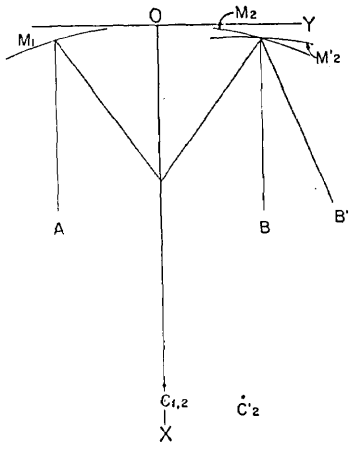


FIG. 2. The mirror surface $M_1$ is tangent to the OY axis at O, hence its center of curvature is at $C_{1,2}$ on the OX axis. For an Ebert system, i.e., a concentric Czerny–Turner spectrometer, the mirror surface $M_2$ is tangent to the OY axis at O and its center is at $C_{1,2}$. For a corrected Czerny–Turner spectrometer by making $R_2<R_1$ such that $\alpha_m\approx\alpha_m'$ a central ray will trace a path similar to the path from A to B; or if one has the condition $\alpha_m<\alpha_m'$ and $R_1\gtrsim R_2$ then a central ray will follow a path similar to the one from A to B'. Under this condition, the mirror surface, $M_2'$ has its center-of-curvature at some point $C_2'$. The central ray shown is parallel to the OX axis; this is not necessary and any path of the central ray from A to $M_1$ to the grating is valid.

Substituting Eqs. (11), (12), (13) into Eq. (14) gives

$$\sin\alpha_m'=R_2^2/R_1^2(\cos\alpha_g\cos\alpha_m'/\cos\beta_g\cos\alpha_m)^3\sin\alpha, \quad (15)$$

or

$$R_2=\left[R_1^2\frac{\sin\alpha_m'}{\sin\alpha_m}\Big/\left(\frac{\cos\alpha_g\cos\alpha_m'}{\cos\beta_g\cos\alpha_m}\right)^3\right]^{\frac{1}{3}}. \quad (16)$$

Equations (15) and (16) may be approximated,

$$\sin\alpha_m'=(R_2^2/R_1^2)(\cos^3\alpha_g/\cos^3\beta_g)\sin\alpha_m, \quad (17)$$

and

$$R_2=R_1(\sin\alpha_m'\cos^3\beta_g/\sin\alpha_m\cos^3\alpha_g)^{\frac{1}{3}}, \quad (18)$$

by ignoring the third-order $\alpha_m$ and $\alpha_m'$ dependence.[15]

Equations (15) through (18) indicate that the symmetrical arrangement normally used in Czerny–Turner spectrometers does not correct coma and that an asymmetrical tilt of the second mirror or change in radius of curvature is needed. The difference between an Ebert spectrometer and a corrected Czerny–Turner spectrometer is shown in Fig. 2.[16]

The difference between the above analysis and Leo's[5] stems from the fact that Leo assumes that $r=R/2$ and we assume the Gaussian off-axis condition $r=(R/2)\cos\alpha_m$. We have also, to a rough approximation, taken into account the effect of coma upon the wavefront curvature after diffraction. Leo[5] assumes a solution of the form $R_1/R_2=\cos\alpha_g/\cos\beta_g$ or $R_2=R_1(\cos\beta_g/\cos\alpha_g)$. If we solve Eq. (18) by setting $\alpha_m=\alpha_m'$ we obtain $R_2=R_1(\cos^{\frac{1}{3}}\beta_g/\cos^{\frac{1}{3}}\alpha_g)$, which is similar to Leo's equation, the difference having been stated previously.

The reduction in the radius of $R_2$ or increase of $\alpha_m'$ is quite adequate when an echellette grating is used; but if an echelle is utilized, $R_2$ is reduced too much and a compromise must be made between increasing $\alpha_m'$ and reducing $R_2$. The best imaging, as will be shown, is when $R_2<R_1$ and $\alpha_m'>\alpha_m$. It is not adequate to let $R_2=R_1$ and $\alpha_m'>\alpha_m$, to correct for coma.

It will be assumed that primary spherical aberration is the only remaining aberration. If $W_1$ is the approximate width of the beam before diffraction we may write for the maximum beamwidth

$$W_1=\left\{64\lambda N\Big/\left[\frac{1}{R_1^3}+\frac{1}{R_2^3}\left(\frac{\cos\beta_{g0}\cos\alpha_m}{\cos\alpha_{g0}\cos\alpha_m'}\right)^4\right]\right\}^{\frac{1}{4}}, \quad (19)$$

where $\lambda$ is the wavelength and $N$ is a number such as 0.25 which will give one the Rayleigh criterion. It should be noted that as the grating angle increases, the effect of spherical aberration due to the second mirror is reduced. Equation (19) will give a good approximation for practical design work.

## V. RESULTS OF CALCULATIONS

When the wavefront aberration is less than about $4\lambda$ or the spatial frequencies are high (the case for medium and high resolution spectrometers) geometrical optics and ray tracing will give little information about the structure of the image and hence of the resolution or contrast at the exit slit; but, since the ray trajectories represent the mean value of the Poynting vectors it is possible to state a relative value relation of spot diagram A to spot diagram B.

All the instruments analyzed have a collimating mirror radius of curvature of 200 cm and normal beamwidth from the collimating mirror of about 14 cm. The off-axis angle of the collimating mirror is 2.58° and the distance from the center of the entrance slit to the edge of the collimated beam is about 2 cm. The angle

[15] G. Rosendahl, J. Opt. Soc. Am. 52, 412 (1962), has derived Eq. (15) without the dependence upon the radii of curvature, by utilizing a different geometrical optic technique. W. G. Fastie (private communication and U. S. Patent 3,011,391) has derived an equation similar to (17) but without the dependence upon the radii of curvature.

[16] W. G. Fastie experimentally noted that the effect of coma may be corrected by tilting the second mirror [Symp. Interferometry, No. 11, 243 (1960), Natl. Phys. Lab., G. Brit.]. The large, high-resolution Ebert spectrometer, which has a focal length of 183 cm [W. G. Fastie, H. M. Crosswhite, and P. Gloersen, J. Opt. Soc. Am. 48, 106 (1958)], achieved a resolving power in excess of 500,000. This was done at an $f$ number $>20$, i.e., a projected grating width $\lesssim 9$ cm. A re-examination of the lines revealed an asymmetry and a coma-like flare (private communication). After a discussion with one of the authors, R. Brower (private communication) of Brower Laboratories, Wellesley Hills, Massachusetts set up a point source, two spherical mirrors, and grating. By using the grating in the zeroth order and aligning the instrument, the effect of coma is eliminated with a symmetrical arrangement; to eliminate the effect of coma for the first or higher orders of diffraction of an echellette grating, the second mirror had to be tilted. When $R_2$ is made $<R_1$, Brower found that the image quality is superior to that with $R_1=R_2$.

between the blaze normal and the incoming or diffracted central ray at the blaze wavelength is about 5.2°; this is larger than usual for a Czerny–Turner monochromator with the above aperture. Normally this angle is about 3°. This has no bearing on the following analysis or comparison between the symmetrical and unsymmetrical Czerny–Turner spectrometer.

### A. Coma Correction

The spot diagram produced by an Ebert system in which the grating angle is 23.2° is shown in Fig. 3(a). This shows the coma and broadening due to diffraction from the grating. Figure 3(b) shows the spot diagram from a Czerny–Turner spectrometer with a grating angle of 23.2° and the second mirror tilted so that the off-axis angle is 3.42°. Figure 3(c) shows the spot diagram for the case in which the radius of curvature of the second mirror is 180 cm and the off-axis angle is 2.62°. In Fig. 4(a) the spot diagram from an Ebert arrangement is shown with a grating angle of 58.3°; the coma is obvious. For the unsymmetric Czerny–Turner spectrometer in Fig. 4(b) the asymmetry through the center of the pattern is corrected absolutely, but the curvature (coma) of the astigmatic pattern is quite large; the off-axis angle of the second mirror is 6.25°. In 4(c) the off-axis angle is 5.15°; the correction is quite good, but to achieve this the central regions of the pattern are displaced to the left and there is a general broadening of the pattern. In Fig. 4(d) the radius of the second mirror is 130 cm and the off-axis angle of the second mirror is 2.7°. The curvature (coma) of the pattern has been reduced.

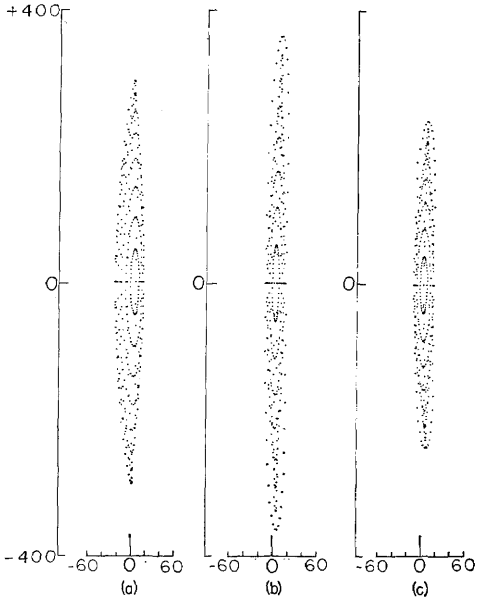


FIG. 3. The above spot diagrams at the exit slit are of a low-blaze Ebert spectrometer (a); a low-blaze Czerny–Turner spectrometer where $R_1=R_2=200$ cm and coma correction is made by increasing the angle $\alpha_m'$ (b); and a Czerny–Turner spectrometer where $R_1=200$ cm and $R_2=180$ cm (c). The coma shown in (a) is reduced in (b) although there is a slight increase of the astigmatism. In both patterns a slight curvature of the astigmatic pattern is noted. The asymmetric Czerny–Turner (c) shows a reduction of both coma and astigmatism. The numerical scale is in microns.

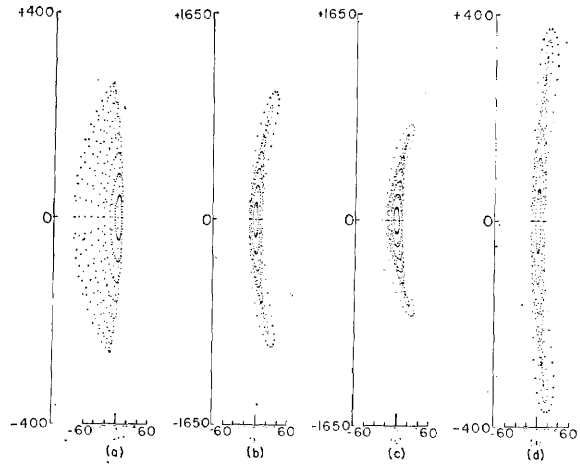


FIG. 4. A comparison of spot diagrams from instruments utilizing high-blaze gratings, hence a steep grating angle; (a) is an Ebert spectrometer; (b) a Czerny–Turner spectrometer where coma is absolutely corrected through the center of the pattern by tilting the second mirror, $R_1=R_2=200$ cm; (c) is the same instrument as (b) except that the tilt of the second mirror has been reduced, bringing coma to the center of the pattern, but partially balancing the diagram; (d) is a Czerny–Turner spectrometer where $R_1=200$ cm and $R_2=130$ cm. The off-axis angle of the second mirror is approximately that of the collimating mirror. Note the change in vertical scale for (b) and (c). In (b) and (c) the curvature of the astigmatic pattern is more pronounced than in the low-blaze case (Fig. 3). The spot diagram (d) indicates that simply tilting the second mirror without a reduction in the radius of curvature will not be a satisfactory correction. All traces originate from the slit center. The numerical scale is in microns.

The curvature of the patterns in Figs. 3(b) and (c) and Figs. 4(b) and (c) is caused by the rays which strike the upper and lower sections of the tilted second mirror and by the astigmatism and spherical aberration from the collimating mirror being transformed by the grating. Equations (15)–(18) indicate that decreasing the radius of curvature of the second mirror will have the same effect as increasing its off-axis angle. It is here, as previously mentioned, that the two dimensional analysis fails.

When a high-blaze grating is used, the ray trace results indicate that a reduction in the radius of the second mirror, such that $\alpha_m \gtrsim \alpha_m'$ and $R_2<R_1$, will be a better imaging condition than simply tilting the second mirror and letting $R_1=R_2$. This may be seen by comparing the spot diagrams of Figs. 3 and 4. The above condition also reduces the astigmatism of the instrument; this shall be discussed in the next section. What effect, if any, reducing the radius of the second mirror will have upon the angular scanning range of the grating has not yet been determined.

The reason that a spectral line would appear to be coma-corrected in an unsymmetric Czerny–Turner spec-

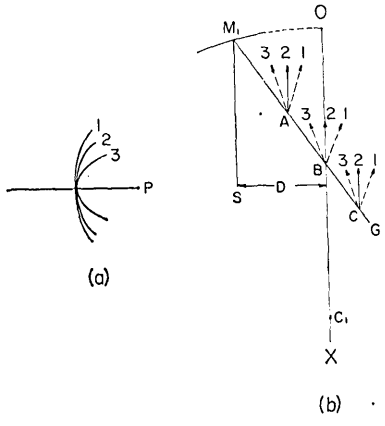


FIG. 5. In (a), (1) is an approximate prolate ellipse, (2) a circle, and (3) an approximate oblate ellipse. They have a common center at point $P$. These curves correspond to the directions of the normal to the blaze step at blaze wavelength shown in (b), $A$, $B$, and $C$. The optical path of $S\,M_1\,G$ is for a central ray striking the grating positioned at $A$, $B$, or $C$ in drawing (b). The central ray is shown parallel to the $OX$ axis as in Fig. 2. But this is not necessary since slit curvature is independent of the trajectory of the central ray from $M_1$ to $G$.

trometer when $R_1=R_2$ and $\alpha_m<\alpha_m'$ is that the integrated effect of a series of asymmetric spot diagrams, such as illustrated in Fig. 4(c), results in an image which contains a symmetrical aberration (spherical aberration).

## B. Astigmatism

It is well known that astigmatism is not corrected in a Czerny–Turner arrangement utilizing two spherical mirrors. The astigmatism is greater for the corrected Czerny–Turner spectrometer where $\alpha_m'>\alpha_m$ and this can be seen in comparing Figs. 3 and 4. Geometrical optics show that this has little effect upon resolution but according to physical optics this may not be correct.

The work of Nienhuis,[17] Van Kampen,[18] and Nienhuis and Nijborn[19] shows that for a circular exit pupil, primary astigmatism produces an asteroid that broadens the diffraction pattern of an astigmatic line. This may be seen in Nienhuis,[17] Born and Wolf,[20] Cagnet, Francon and Thrierr,[21] or Wolf.[22] Whether this is deleterious to medium or high spectral resolution in a spectrometer cannot be determined by geometrical optics. Astigmatism due to the collimating mirror will also have an asymmetric effect upon the diffracted wavefront [see Secs. III and V(a)].

[17] K. Nienhuis, thesis, University of Groningen, 1948.
[18] N. G. Van Kampen, Physica **15**, 575 (1949).
[19] K. Nienhuis and B. R. A. Nijborn, Physica **15**, 590 (1949).
[20] M. Born and E. Wolf, *Principles of Optics* (Pergamon Press Inc., New York, 1959), p. 477.
[21] M. Cagnet, M. Francon, and J. C. Thrierr, *Atlas of Optical Phenomena* (Springer-Verlag, Berlin, 1963).
[22] E. Wolf, Rept. Progr. Phys. 14, 95 (1951).

## C. Slit Curvature

The slit curvature for an instrument is obtained numerically by iterative techniques which determine the radius of curvature of the slit, if circular, measured from the axial line $OX$ [see Figs. 2 and 5(b)], the major and minor axes of an ellipse whose center lies on a line through the grating and is parallel to the $OX$ axial line or whose center lies on the $OX$ axial line, and all pertinent data so that a ray trace may proceed from any point on the calculated slit curve.

The general results of our calculations of slit curvature for several instruments are: (a) slit curvature is a function of the distance from the entrance slit to the collimating mirror; for best imagery, this distance is not necessarily equal to the focal length of the mirror for any type of Czerny–Turner orientation.[23] Slit curvature is also a function of orientation of the normal to the blaze step at the blaze wavelength to the axial line $OX$ [Fig. 2 and Fig. 5(b)]; (b) slit curvature may be any type of second degree curve determined by the above; (c) under the condition that $0<\chi<\pi/4$ and that the best focusing condition has been chosen, the curve approximates an ellipse. The approximate ellipse degenerates to a circle when the blaze normal at blaze wavelength is parallel to the $OX$ axis. This is the well-known Fastie slit.[2]

In Fig. 5(a) the circular slit (No. 2) is shown and the

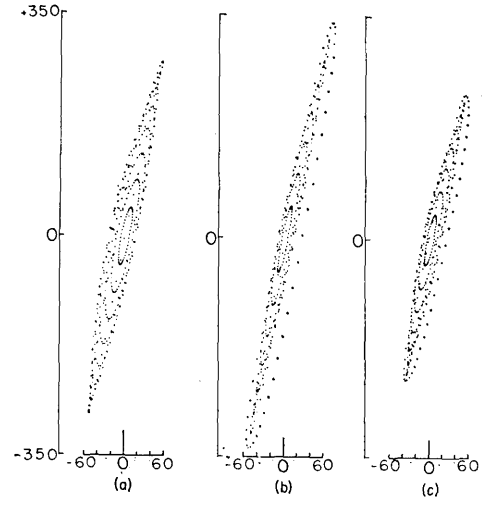


FIG. 6. These spot diagrams all originate from 2.75 cm above the center of a circular slit. This would be a slit length of 5.5 cm. They are for low-blaze grating instruments; (a) is an Ebert spectrometer; (b) is a Czerny–Turner where $R_1=R_2=200$ cm, and (c) is a Czerny–Turner spectrometer where $R_1=200$ cm and $R_2=180$ cm. The comatic shift towards the right, as compared to Fig. 3 is quite pronounced and, as explained in the text and Fig. 7, limits the slit length. The numerical scale is in microns.

[23] To illustrate the sensitivity of the slit curvature upon the distance from the entrance slit to the collimating mirror: for one of the instruments analyzed, a shift of 0.3 mm distorted the slit curvature from a circle to a smooth curve which deviates from a circle by $\approx 6\,\mu$ at the slit center to $\approx 0.2\,\mu$, 2.75 cm above or below the slit center.

approximate prolate and oblate elliptical slits (Nos. 1, and 3, respectively) are shown. The elliptical character of the slit was predicted by Kudo,[4] but not generalized as to grating position.

It makes no difference where the grating is located along the path $M_1$ to $G$ as illustrated in Fig. 5(b). The positions of the center of the grating $A$, $B$, and $C$ have no effect upon slit curvature; the orientation of the blaze normal at the blaze wavelength numbers 3, 2, and 1 is critical. These numbers correspond to the curve numbers in Fig. 5(a); of course, the grating should be positioned nearly telecentric on the object side, to reduce vignetting.

The center of the slit curve always lies on the $OX$ axis, under the condition that the mirror surface is tangential to the $OY$ axis, Figs. 2 and 5(b), at the point $O$. This is the Ebert condition; to build a Czerny–Turner spectrometer with circular slits, the center of curvature of the collimating mirror must lie on the $OX$ axis at $C_1$. The position of the second mirror is arbitrary and is a function of optical or mechanical requirements. Figure 5(b), shows the distance $D$ from the axis to the center of the slit, and is in all cases the distance from the center of the slit curve to the center of the slit. In Fig. 5(a) this is the distance from $P$ to the slit center, where the three curves have a common tangent point.

Preliminary work on an exact, analytic expression for slit curvature indicates that the slit curvature, as a function of the blaze normal, goes through all the conic sections from a point through an ellipse, circle, ellipse, parabola, hyperbola, and finally a straight line, as the angle $\chi$ varies from zero to $\pi/2$. The effect of slit length upon aberration is illustrated in Figs. 6(a), (b), and (c) and Figs. 7(a), (b), and (c).

In comparing the three low-blaze instruments one can see that as a point source moves up the entrance slit, the direction of the coma is to the right. If there is correction for coma in a small region near the center of the slit, the coma is not corrected at a point above or below the slit center. The coma as a function of slit length is schematically illustrated in Fig. 7.

If $R_1 \neq R_2$, the radius of the exit slit is simply $(R_2/R_1)$ $\times$(radius of the entrance slit).

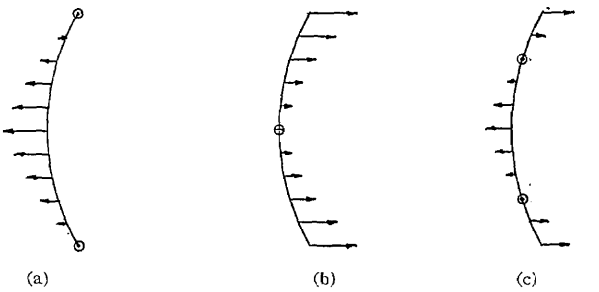


FIG. 7. This schematically illustrates a general curve for the exit slit. The arrows show the direction of coma, length is indicative of the amount and zeros show the points of coma correction. Curve (a) is for a high-blaze symmetrical arrangement or a low-blaze symmetrical arrangement with large angle ($\chi$). It shows the large amount of coma near the central region and decrease towards the slit ends. Curve (b) is for a high- or low-blaze unsymmetrical arrangement in which there is absolute coma correction near the slit center, e.g., aligning the instrument by imaging a point source. The coma increases towards the slit ends. Curve (c) represents a symmetric arrangement of low-blaze angle and small angle ($\chi$), an unsymmetric, low blaze arrangement with large angle ($\chi$), or a high-blaze, unsymmetric arrangement. Coma is introduced near the slit center and is balanced towards the ends.

## VI. COMPARISON WITH OTHER INSTRUMENTS

If one compares the luminosity[8–11,13] (defined as $\Phi/B_\lambda$, see Sec. II) of the various types of grating spectrometer-monochromators now in use to the Czerny–Turner monochromator, symmetric or asymmetric, the Czerny–Turner monochromator will be superior. The Ebert spectrometer (concentric, symmetrical Czerny–Turner spectrometer) has been used for some time with gratings whose blaze is $\approx 60°$. To achieve good resolution, the width of the exit pupil (aperture) must be reduced from any theoretically calculated value. If a grating which has a blaze angle of 76° is used in an Ebert system a further reduction in aperture would be required to maintain good resolution.[16]

The Fabry–Perot spectrometer[8,9,12,13,24,25] has a definite luminosity advantage whenever the resolving power is $\geq 10^6$ over the large, high-blaze grating Czerny–Turner spectrometer. The resolving power of a grating may be written as $R=\lambda/\delta\lambda \approx 2(W/\lambda)\sin\varphi\cos\chi$. The flux passing through a spectrometer using a grating of width $\approx 25$ cm would be severely limited if $R \sim 10^6$. The factor $k$ (see Sec. II) would be $\sim 0$. In the ultraviolet, 1000 Å $\lesssim\lambda\lesssim$ 4000 Å, and infrared, 1 $\mu \lesssim \lambda \lesssim 25\,\mu$, the Fabry–Perot spectrometer presents technical problems of coatings, plate fabrication and scanning methods which must be brought into any comparison with the Czerny–Turner spectrometer. The visible is the best region of the spectrum for comparison, since this is advantageous to the Fabry–Perot spectrometer. A valid comparison may then be made when $R < 10^6$.

Without going into detail on the theory of the Fabry–Perot spectrometer, the equation which describes the luminosity of a Fabry–Perot etalon is $L_F = A_F \Omega \tau$, where $A_F$ is the utilized area of the plates, $\Omega$ is the solid angle, and $\tau$ is a transmittance. The transmittance, $\tau$, results from the product of three transmittances, $\tau_A$, $\tau_F$, and $\tau_E$. Under near-optimum conditions $\tau_E \approx 0.8$, $\tau_F \approx 0.8$, and $\tau_A \lesssim 0.75$ (a good seven-layer coating of ZnS–$Na_3AlF_6$ will have $\tau_A \approx 0.7$).[24]

From the above and from the geometry of the Fabry–Perot etalon, we may write for the luminosity of a single etalon $L_F \approx 1.5 A_F/R$, where $R$ is the resolving power. From Sec. II, the luminosity of the Czerny–Turner spectrometer may be written as

[24] J. E. Mack, D. P. McNutt, F. L. Roesler, and R. Chabbal, Appl. Opt. 2, 855 (1963).

[25] R. G. Greenler, J. Opt. Soc. Am. 47, 642 (1957).

$L_G = 2k\tau\beta A_G \sin\varphi \cos\chi/R$. We shall assume that $k=0.75$, $\tau=0.6$, $\beta=0.04$, $\sin\varphi=0.97$, and $\cos\chi\sim 1$. The luminosity of the Czerny–Turner spectrometer will then be $L_G \approx 0.04(A_G/R)$ where $A_G$ is the area of the grating. On the basis of equal resolving power, the luminosity ratio of the Fabry–Perot etalon to the Czerny–Turner spectrometer is then $\approx 50(A_F/A_G)$.

When two or three etalons (the third and fourth etalons may be interference-absorption filters[24,25]) are added to the optical train to make a Fabry–Perot spectrometer, reduction in luminosity due to further absorptance by the coatings, ghost rejection, reflection losses, and automasking must be considered. The luminosity ratio will then be $\gtrsim(A_F/A_G)$ to $\gtrsim 10(A_F/A_G)$.

From the preceding it may be inferred that in most cases a high-blaze grating Czerny–Turner spectrometer has superior luminosity; Stroke[10] has made a similar observation.

In the infrared, $1\ \mu \lesssim \lambda \lesssim 25\ \mu$, the detector noise, at present, is greater than the statistical photon noise i.e., signal noise. In this region of the spectrum a Michelson interferometer, making use of the Fourier transform techniques, has a signal/noise advantage over the large, high-blaze grating Czerny–Turner spectrometer.[26] If infrared detectors could be made such that the noise equivalent power is $<10^{-12}$ W, this advantage would be partly eliminated. In the wavelength region $4\ \mu \lesssim \lambda \lesssim 13\ \mu$ and for weak sources of radiation, we must also consider blackbody photons from the spectrometer and chopper. This is an added photon noise and can be serious. In this spectral region centered near $9\ \mu$, no matter how good the detector, the superiority of the Michelson interferometer may well remain.

A similar argument may be used to compare modulating spectrometers such as Connes' SISAM[13,27] or Girard's grille spectrometer[28,29] to the Czerny–Turner monochromator. We shall refer only to Girard's grille spectrometer, since both are modulating spectrometers.

It may be of interest to compare the instrument from Ref. 29 which has a focal length of 200 cm to a Czerny–Turner spectrometer-monochromator. The Czerny–Turner may have a luminosity increase of $\approx 2$ to 45 by using a high-blaze echelle. The Girard grille has an aperture width of $\approx 16.9$ cm; the Czerny–Turner will work at the wavelength involved with an aperture of $\approx 25$ cm. This is an increase in luminosity of $\approx 2$. The length of the central grille in the grille spectrometer is 3 cm, whereas in the Czerny–Turner the slit length can be 8 to 9 cm; this provides an increase of luminosity of $\approx 3$. The total factor of luminosity increase is then 8 to 180. There is a factor of $\approx 130$ increase in the arrangement of Girard's instrument as compared to his instrument used as a monochromator. The luminosity advantage of the grille spectrometer over the Czerny–Turner monochromator is then from $\approx 16$ to 0.7. If the $f$ number is to be maintained, the above comparison is not realistic, since a high blaze grating in the Czerny–Turner spectrometer would have a width of $\sim 50$ cm. The maximum attainable width is $\approx 25$ cm. If an echelle of 25 cm were used, the luminosity advantage of the grille spectrometer would be $\sim 6$. The previous comparison of luminosity advantage of $\sim 1$ would be quite valid if a focal length $\gtrsim 100$ cm were used.

In the Girard grille spectrometer only the modulated wavelength is detected as signal, but a large part of the spectrum on either side of the modulated wavelength is detected as statistical photon noise. The photon noise is more serious to the Girard grille than to a Michelson interferometer since the Girard grille detects one spectral element at a time instead of all the spectral elements simultaneously; hence, in the infrared near $9\ \mu$ and using weak sources of radiation, the Czerny–Turner spectrometer should be far superior to the Girard grille.

Only if the Littrow system of Girard will allow the use of a high-blaze grating, longer grille slits, and larger aperture, will the luminosity gain of the grille spectrometer be a factor of 130 greater than a Czerny–Turner monochromator.[30]

## VII. DISCUSSION

The use of high-blaze gratings in conjunction with the asymmetric Czerny–Turner arrangement should produce a luminosity increase over a symmetrical system such that it is quite comparable to interferometric and modulating devices. The use of spherical mirrors for collimating and condensing makes it relatively simple and economical to build.

For large apertures the resolution limit will not be defined by diffraction, but from the residual coma (Sec. V and Fig. 4).

The above suggests that an investigation as to the feasibility of using aspherical mirrors for collimating and/or condensing may prove worthwhile; but care should be taken, for an analysis which only considers the image quality of one point source is rather useless. The luminosity is proportional to the slit length; hence, several points along a slit should be considered.

As was explained in Sec. IV, the relative optimum relationship of the grating angle, radius of the second

[26] We shall be interested only in resolution $\leq 1\ \text{cm}^{-1}$ in the above stated wavelength region. This value of resolution, to the author's knowledge, has not been achieved by interferometers employing the Fourier transformation techniques. In the spectral region where photomultiplying tubes can be used as detectors ($\lesssim 1\ \mu$) the signal/noise advantage of these types of interferometers is nullified. The argument shall proceed under the assumption that higher resolution will be obtained in the future.

[27] J. Connes, J. Phys. Radium 19, 197 (1958); Symposium on Interferometry, National Physics Laboratory, Great Britian No. 11, 409 (1960).

[28] A. Girard, Opt. Acta, 7, 81 (1960).

[29] A. Girard, Appl. Opt. 2, 79 (1963).

[30] G. Stroke (private communication) informed us that he gave Girard a grating blazed at 45°. Evidently Girard did not use it in the previous referenced papers since the scanning range was $37° < \theta < 22°$ in a Littrow system. If the grille spectrometer is used with a grating of 45° blaze angle, then the luminosity advantage of the grille spectrometer over the Czerny–Turner monochromator would be $\approx 30$ to 1.3.

mirror ($R_2$) and the off-axis angle of the second mirror ($a_m'$) has not been solved; and until this is done it will not be a simple matter to optimize completely the design of the asymmetric Czerny–Turner spectrometer.

A grating blaze angle of 76° has been used throughout, when flux or luminosity were calculated. A blaze angle of 64° would make little difference in the result of comparison; in fact, this angle was used for the initial calculations, but was changed after reading Stroke[10] under the assumption that this type of grating may soon be available.

ACKNOWLEDGMENTS

The authors are greatly indebted to Professor H. N. Rundle, University of Saskatchewan, who, while at the National Bureau of Standards, Boulder, Colorado, acted as a responsive sounding board and excellent critic. The authors also wish to thank Jack W. Stunkel, Walter Harrop, David Hansen, A. V. Brackett, and Alice Keysor for their assistance.

We would like to thank Dr. D. M. Gates without whose support this paper could not have been completed.

JOURNAL OF THE OPTICAL SOCIETY OF AMERICA VOLUME 54, NUMBER 7 JULY 1964

# Resonant Modes of Optic Interferometer Cavities. I. Plane-Parallel End Reflectors*

LEONARD BERGSTEIN AND HARRY SCHACHTER

*Department of Electrical Engineering, Polytechnic Institute of Brooklyn, Brooklyn, New York 11201*

(Received 7 November 1963)

A study is made of the resonant or normal modes of optic and quasioptic interferometer cavities with plane-parallel end reflectors. The solution of the integral equation governing the relation between the normal modes and the geometry of the cavity is found by means of a series expansion of orthogonal functions. The terms of the series for the normal modes can be interpreted as Fraunhofer diffraction patterns characteristic of the geometry of the end reflectors. Various geometries, such as the infinite-strip, rectangular, and circular end reflector cavities, are considered and the results plotted and interpreted.

## I. INTRODUCTION

FABRY–PEROT interferometers are used extensively as infrared and optical maser (or laser) resonators. The interferometer consists essentially of two highly reflecting plane surfaces facing each other and separated by a fixed distance. An active medium is immersed in the region between the reflectors. An electromagnetic wave leaving one of the reflecting surfaces will be amplified as it propagates through the active medium toward the other reflecting surface. At the same time, there will be a decrease in the intensity of the wave due to scattering by inhomogeneities in the medium. A further decrease in the intensity will be caused by the diffraction spread of the wave. When the wave arrives at the other end of the resonator additional power will be lost in reflection due to the finite conductivity and/or partial transmission of the reflector. For power-buildup (oscillations) to occur in the resonator, the total power loss must be less than the power gained by travel through the active medium. The relative scattering and reflection losses (i.e., the ratio of the power losses per unit cross-section area over the field intensity) are constant and depend only on the homogeneity of the interferometer medium and the reflector properties, respectively. The diffraction losses, however, depend on the field distribution within the interferometer. They thus determine not only the start-oscillation condition but also the field distribution in the interferometer during oscillations. For an arbitrary initial field distribution, the diffraction losses will cause shifts in the distribution from reflection to reflection until a self-reproducing field distribution, if one exists, will be set up. These steady-state distributions or normal modes must be independent of the initial disturbance and are properties of the geometry of the end reflectors only. The relation between the geometry of the end reflectors and the field distribution of these normal modes, the diffraction losses associated with them, and the resonant frequencies of these modes are of interest in understanding the operation of masers using Fabry-Perot interferometers as resonant cavities. Furthermore, from the distribution of the electromagnetic field within the interferometer, we can determine the field distribution of the emerging beam, its angular spread, and the maximum intensity that can be achieved by means of a focusing lens.

Schawlow and Townes[1] concluded that the Fabry–Perot cavity is resonant to uniform plane waves travel-

* The work reported here is part of a dissertation submitted by H. Schachter in partial fulfillment of requirements for the Ph.D. degree at Polytechnic Institute of Brooklyn. The work was supported by the Joint Services Technical Advisory Committee under Office of Aerospace Research Grant AF-AFOSR-453-63.

[1] A. L. Schawlow and C. H. Townes, Phys. Rev. **112**, 1940 (1958).